Nonlinear Dynamics and Systems Theory, **6** (4) (2006) 367–387

Deterministic Chaos in a System Generator – Piezoceramic Transducer

T.S. Krasnopolskaya [1] and A.Yu. Shvets [2*]

[1] *Institute of Hydromechanics, National Academy of Sciences of Ukraine, 03057, Zheljabova Str., 8/4, Kyiv, Ukraine*
[2] *NTUU Kyiv Polytechnic Institute, 03057, Pobedy ave., 37, Kyiv, Ukraine*

Received: January 11, 2006; Revised: September 28, 2006

Abstract: New models and properties of piezoceramic transducer due to the interaction with the excitation device of limited power-supply are built and investigated in details. The special attention is given to examination of origin and development of the deterministic chaos in this system. It is shown, that a major variety of effects typical for problems of chaotic dynamics is inherent in the system. The presence of several types of chaotic attractors is established and the existence of hyper-chaos is revealed. Various scenarios of passage from the regular regimes to chaotic are explored. Explicitly phase portraits and Poincaré sections and maps of of chaotic attractors are investigated. Their spectral densities and distributions of invariant measures are obtained and explored.

Keywords: *Limited excitation; piezoeffect; chaotic attractor; Lyapunov exponents; Poincaré section and mapping.*

Mathematics Subject Classification (2000): 37D45, 37G35, 37L30, 74B99.

1 Introduction

Functioning of many important and mission-critical devices of various engineering machines, including transformers, is based on the effect of coupling of mechanical and electrical fields in piezoceramic media [2, 3, 8, 26, 27, 28, 23]. Hence, creation of a general mathematical theory of electroelastic processes in such media under arbitrary conditions of mechanical and electrical loading is important, both in scientific and applied aspects. Such theory for many piezoceramic devices and constructions is created by A.F. Ulitko and his school [3, 8, 26, 27, 28]. However, in these theories, and in other publications, a problem of behaviour of electroelastic fields is considered only for conditions of forced

* Corresponding author: alex.shvets@bigmir.net

and free oscillations, when the piezoelectric ceramics is under the action of applied mechanical and electrical fields of given values. Thus a problem of influence of dissipation and radiation of energy under oscillations of coupled fields of the device remains outside of many considerations. If the transducer with electroelastic coupled field is mounted in a medium with resistance, as happens in operation of sound emitters, then radiation of energy changes an electric field in the power generator, as opposed to the "ideal" case when no losses occur happen. This adjustment can be essential and lead to unexpected dynamic conditions or be negligibly small — it depends on outer power of the generator compared as with an emitting power. Examination of new effects in dynamics of piezoceramic coupled fields and in functioning of the power generator, which are caused by "sensitivity" of cumulative systems to radiation of energy is, without a doubt, of significant scientific interest. This is a case of so-called limited or non-ideal excitation [12, 24, 25] when supply power is of the same order as the power consumed by a loading piezoceramic transducer. In this case the electric generator is said to have limited power, i.e. a power comparable with the power radiated or consumed by piezoceramic coupled field. The present paper is devoted to the analysis of interaction effects, collectively called the effect of Sommerfeld–Kononenko [12, 13, 15, 16, 17, 18, 19, 24, 25], in oscillations of the piezoceramic transducer and in the mechanism of its excitation — the generator of the electric current of limited power-supply. A new mathematical model of interaction of the generator and the piezoceramic transducer submerged in a hydromedium with resistance is constructed. The coupling of processes in the transformer and the energy source (the generator) leads to the qualitatively new effects in their dynamics that cannot be seen using a model of the problem with unlimited or so-called "ideal" excitation — primarily the possibility of appearance of deterministic chaotic regimes, which are theoretically impossible in a problem with ideal excitation (when corresponding mathematical models of such a problem have dimensionality of phase spaces equal to two, a possibility of chaos origination is excluded).

2 Construction of a mathematical model

Let us consider a piezoceramic rod transducer, which is loaded on the acoustic medium and to which electrodes the electrical voltage is affixed, raised by the LC–generator (Figure 2.1). The selection of the generator of such type is caused by the renaissance of its application observable now in the up-to-date technique. This is related with facts that the electrovacuum-tube (analogue) devices ensure higher metrological characteristic on to comparison with the numeral devices. The origin of the Cartesian coordinate system is in the middle of the rod; from its surfaces S_- and S_+, which are perpendicular to axis oz, acoustic signals radiate into the medium. We will examine the longitudinal vibrations of a round rod of length $2h$ and cross-sectional area S, with longitudinal polarization.

According to the theory of longitudinal deformations [8, 27] the piezoeffect constitutive relations have the form

$$\epsilon_z = s_{33}\sigma_z + d_{33}E_z, \qquad D_z = \epsilon_{33}E_{,z} + d_{33}\sigma_z, \tag{1}$$

where ϵ_z is a longitudinal deformation; σ_z is the mechanical stress; E_z is the intensity of the electric field; D_z is an induction of this field; and $s_{33}, d_{33}, \epsilon_{33}$ are constants.

When studying the acoustic frequency region, we used the equations of a quasistatic

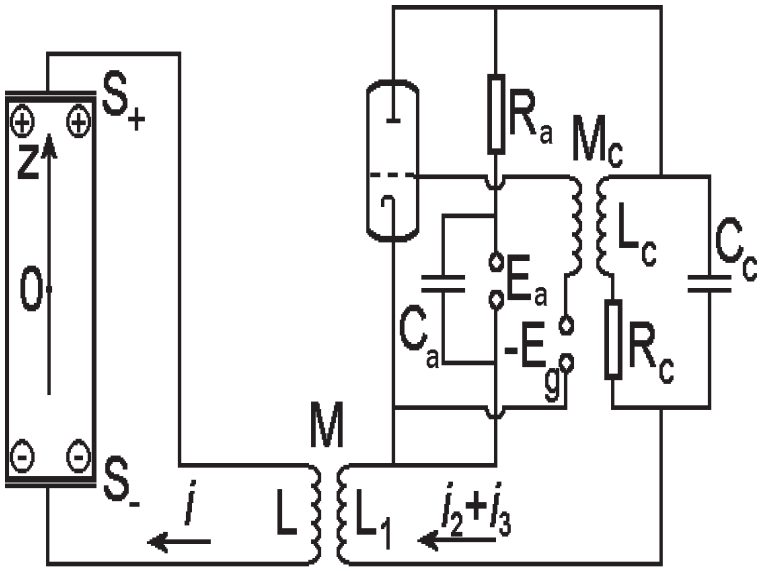

Figure 2.1: Scheme of viewed system.

field. Here, they could be written as

$$\frac{\partial D_z}{\partial z} = 0, \qquad E_z = -\frac{\partial \Psi}{\partial z}, \tag{2}$$

where Ψ is an electrical potential.

We shall add to equations (1)–(2) the Cauchy relation $\epsilon_z = \dfrac{\partial u}{\partial z}$ and the equation of the rod vibrations

$$\frac{\partial \sigma_z}{\partial z} = \rho \frac{\partial^2 u}{\partial t^2}, \tag{3}$$

where $u = u(z,t)$ is the longitudinal displacement of the rod, ρ is its density.

The boundary conditions, when the rod is under an acoustic load impedance η_0, are as follows

$$\sigma_z = -\eta_0 \frac{\partial u}{\partial t}, \qquad \Psi = \pm V(t), \qquad z = \pm h. \tag{4}$$

The voltage in the electrodes of the rod is $2V(t)$. It is a known function of time in the problem of "forced" vibrations of the transducer and "unlimited" power from the generator. The system of equations (1)–(4) represents a complete description of "forced" vibrations with ideal excitation, when $2V(t)$ is a harmonic function of time. But $2V(t)$ is the voltage in a real physical circuit and a current

$$i = -\frac{\partial (S_z)}{\partial t}$$

flows through the rod. The current i of the transformer with the rod is related with a current of the generator $i_2 + i_3$ according to the differential equation

$$2V + L\frac{di}{dt} = M\frac{d(i_2 + i_3)}{dt}. \tag{5}$$

For comparison we may present this relation for the case of the absence of the rod, namely

$$L\frac{di}{dt} = M\frac{d(i_2+i_3)}{dt}.$$

So, the presence of the rod in the circuit changes the disturbance to the voltage in every part of the circuit. The addition of a rod is like the addition of some capacity (the input electrical impedance at the rod transducer can be calculated to some approximation from so - called geometrical capacity) [2]. We must have a different value i for the circuit with the transducer as compared with that without it. If i is small and $2V \gg L\frac{di}{dt}$ (in this case, $2V \approx M\frac{d(i_2+i_3)}{dt}$) then we have an ideal excitation of the transducer. When $2V$ is comparable with $L\frac{di}{dt}$, the statement does a given value of $2V(t)$ not hold about, because i will also influence regimes of the generator through a transformer (i influences the current i_2+i_3).

A vacuum-tube generator is the classical example of a self-exciting system [21]. Let us write Kirchhoff's equations for each branch of the tube generator current [13, 15]. First of all we assume, that the generator works in the soft condition, i.e.

$$i_a = I_0 + I_1(e_g + De_a) - I_3(e_g + De_a)^3, \tag{6}$$

where i_a is the anode current, e_g is the tube grid voltage; e_a is the anodic voltage; D is the penetration factor of the tube; I_0, I_1, I_3 are constant parameters of the tube.

The equations of currents of the generator are

$$\begin{gathered} i_a = i_1 + i_2 + i_3, \quad e_a - E_a + R_a i_1 = 0, \quad e_g + E_g - M_c\frac{di_2}{dt} = 0, \\ L_c\frac{di_2}{dt} + R_c i_2 = \frac{1}{C_c}\int i_3\,dt, \\ e_a + L_c\frac{di_2}{dt} + R_c i_2 + L_1\frac{d(i_2+i_3)}{dt} = 0. \end{gathered} \tag{7}$$

The system of equations (6)–(7) describes interior processes in a vacuum-tube generator. These equations are nonlinear with respect to e_g (usually D is a small value), we can reduce them to a single equation. Introducing a new variable

$$\phi(t) = \int_0^t (e_g - E_g)dt \tag{8}$$

(here $-E_g$ is the constant component of the voltage e_g), we obtained the following nonlinear equation for the function ϕ

$$\frac{d^2\phi}{dt^2} + \omega_0^2\phi = a_1\frac{d\phi}{dt} + a_2\left(\frac{d\phi}{dt}\right)^2 - a_3\left(\frac{d\phi}{dt}\right)^3, \tag{9}$$

where

$$a_1 = \frac{M_c}{L_cC_c}\left[I_1 - \frac{R_cR_aC_c - L_c}{R_a(M_c - DL_c)} + \frac{R_cL_1}{R_a^2M_c} - 3I_3(E_g)^2\right], \quad a_2 = 3\frac{M_cI_3E_g}{L_cC_c}, \quad a_3 = \frac{M_cI_3}{L_cC_c}.$$

Besides

$$\omega_0^2 = \frac{R_a + R_k}{R_a L_k C_k}$$

and ω_0 is a frequency of the generator in the linear theory.

If the generator is connected to the electric circuit of the transformer, the last equation of the system (7) changes to the following

$$e_a + L_c \frac{di_2}{dt} + R_c i_2 + L_1 \frac{d(i_2 + i_3)}{dt} = M \frac{di}{dt}. \tag{10}$$

Now for inner processes in the generator a such new equation for the function ϕ should be fulfilled

$$\ddot{\phi} + \omega_0^2 \phi = a_0 \dot{\phi} + a_2 \dot{\phi}^2 - a_3 \dot{\phi}^3 - a_4 V(t), \tag{11}$$

where

$$a_0 = a_1 - \frac{M^2 R_c}{L_c C_c L R_a^2}, \quad a_4 = \frac{2MM_c}{LR_a L_c C_c}.$$

Thus, the operation of the generator and the creation of a voltage $2V(t)$ are described not by the equation (9), but by the system of fourth order equations (11) and (5), where the value of i depends on the mechanical deformations of the rod.

For such deformations and the electric field we have the following system of equations

$$c^2 \frac{\partial^2 u}{\partial z^2} = \frac{\partial^2 u}{\partial t^2}, \quad \frac{\partial^2 \Psi}{\partial z^2} = \frac{k^2}{d_{33}(1-k^2)} \frac{\partial^2 u}{\partial z^2}, \tag{12}$$

where $c = [\rho s_{33}(1-k^2)]^{-1/2}$ is a velocity of longitudinal conjugate waves in the rod; $k = d_{33}(\epsilon_{33} s_{33})^{-1/2}$.

Let's present longitudinal oscillations of the rod in the form of the sum of eigenmodes, namely [22]

$$u(z,t) = \sum_{i=1}^{N} f_i(t) \sin \mu_i z. \tag{13}$$

Here μ_i is a solution of the equation $\mu_i h \cos \mu_i h - k2 \sin \mu_i h = 0$.

In this case for the voltage Ψ we shall have [2]

$$\Psi(z,t) = f(t) z + \frac{k^2}{d_{33}(1-k^2)} \sum_{i=1}^{N} f_i(t) \sin \mu_i z. \tag{14}$$

Thus the current i, flowing through the rod is equal to

$$i = -\frac{\partial (S D_z)}{\partial t} = S\epsilon_{33}(1-k^2)\dot{f} = S\epsilon_{33} \frac{(1-k^2)}{h} \left[\dot{V} - \frac{k^2}{d_{33}(1-k^2)} \sum_{i=1}^{N} \dot{f}_i \sin \mu_i h \right]. \tag{15}$$

Using boundary conditions (4), we obtain the following relations for eigenmodes of oscillations

$$-\frac{s_{33} h \eta_0}{d_{33}} \sum_{i=1}^{N} \dot{f}_i(t) \sin \mu_i h = V(t) \tag{16}$$

and

$$i = \frac{S\epsilon_{33}(1-k^2)}{h} \dot{V}(t) + \frac{\epsilon_{33} k^2}{h^2 \eta_0} V(t). \tag{17}$$

Substituting these expressions in (5), we find that voltage $2V(t)$, applied to the electrodes of the transducer should be determined as the solution of the system of equations

$$\begin{aligned} \ddot{\phi} + \omega_0^2\phi &= a_1\dot{\phi} + a_2\dot{\phi}^2 - a_3\dot{\phi}^3 - a_4V(t), \\ \ddot{V}(t) + \omega_1^2V(t) &= a_5\phi + a_6\dot{\phi} - a_7\dot{V}(t). \end{aligned} \tag{18}$$

Here

$$\omega_1^2 = \frac{2h}{LS\epsilon_{33}(1-k^2)}, \quad a_5 = -\frac{M\omega_1^2R_c(R_a+R_c)}{2M_cR_aL_c}, \quad a_6 = -\frac{M\omega_1^2R_c}{2M_cR_a}, \quad a_7 = \frac{k^2}{\eta_0hS(1-k^2)}.$$

After the determination of $V(t)$, longitudinal oscillations of the rod $u(t) = \sum_{i=1}^{N} f_i(t)\sin\mu_i z$ are defined by the following equation

$$\frac{\partial^2u}{\partial t^2} = c^2\frac{\partial^2u}{\partial z^2} - \frac{d_{33}}{s_{33}h\rho}V(t)\delta(z-h) + \frac{d_{33}}{s_{33}h\rho}V(t)\delta(z+h), \tag{19}$$

where $\delta(z)$ is the delta-function.

If we neglect the inverse influence of transducer oscillations (mechanical and electrical) on functioning of the generator ($a_4 = 0$), in other words, if we neglect the effect of Sommerfeld - Kononenko, the system of equations (18) breaks up into two equations, each of which has dimension of a phase space equal to two. First of them is the self-exciting equation and can be solved irrespectively of the second. The second equation, featuring vibrational processes in the rod, is linear. In this case possible attractors of the system of equations (18) always are the regular one. Therefore, in this situation functioning of the generator and radiation of waves by the transducer in acoustic medium correspond to regular (probably complex enough) processes.

If $a_4 \neq 0$, dimension of a phase space of the equation system (18) is equal to four. In this case in the system both regular, and chaotic attractors can exist [14, 21, 20]. Thus, the basic possibility of existence of chaotic regimes in the generator and excitation of chaotic waves in acoustic medium is caused by the effect of Sommerfeld–Kononenko.

3 Investigation of the steady-state regimes of interaction

For determination of the possible steady-state regimes of interaction in the system (18) we use the dimensionless variables

$$\xi = \frac{\phi\omega_0}{E_g}, \quad \frac{d\xi}{d\tau} = \zeta, \quad \beta = \frac{V}{E_g}, \quad \frac{d\beta}{d\tau} = \gamma, \quad \tau = \omega_0 t. \tag{20}$$

Then the system of equations (18) can be written in the form

$$\begin{aligned} \frac{d\xi}{d\tau} &= \zeta, \quad \frac{d\zeta}{d\tau} = -\xi + \alpha_1\zeta + \alpha_2\zeta^2 - \alpha_3\zeta^3 + \alpha_4\beta, \\ \frac{d\beta}{d\tau} &= \gamma, \quad \frac{d\gamma}{d\tau} = \alpha_5\xi + \alpha_6\zeta - \alpha_0\beta - \alpha_7\gamma, \end{aligned} \tag{21}$$

where the coefficients are equal to

$$\begin{aligned} \alpha_0 = \frac{\omega_1^2}{\omega_0^2}, \quad \alpha_1 = \frac{a_0}{\omega_0}, \quad \alpha_2 = \frac{a_2E_g}{\omega_0}, \quad \alpha_3 = \frac{a_3E_g^2}{\omega_0}, \\ \alpha_4 = -\frac{a_4}{\omega_0}, \quad \alpha_5 = \frac{a_5}{\omega_0^3}, \quad \alpha_6 = \frac{a_6}{\omega_0^2}, \quad \alpha_7 = \frac{a_7}{\omega_0}. \end{aligned}$$

First of all we investigate equilibrium states of the system (21). All of them are defined as solutions of non-linear algebraic coupled equations

$$\begin{aligned} &\zeta = 0, \quad -\xi + \alpha_1\zeta + \alpha_2\zeta_2 - \alpha_3\zeta_3 + \alpha_4\beta = 0, \\ &\gamma = 0, \quad \alpha_5\xi + \alpha_6\zeta - \alpha_0\beta - \alpha_7\gamma = 0. \end{aligned} \tag{22}$$

At realization of the requirement $\alpha_0 = \alpha_4\alpha_5$ this system has the infinite set of solutions which are defined by the formulas

$$\zeta = 0, \quad \xi = \alpha_4\beta, \quad \gamma = 0, \quad \beta = r,$$

where r is any real number not equal to zero. At realization of the requirement

$$\alpha_0 \neq \alpha_4\alpha_5 \tag{23}$$

the system (22) has the single trivial solution $\xi = 0, \quad \zeta = 0, \quad \beta = 0, \quad \gamma = 0$. This solution corresponds to the zero equilibrium state, which at realization of a requirement (23), will be a single equilibrium state of the system.

According to the criterion of Hurwitz, sufficient conditions for asymptotic stability of a zero equilibrium state can be written in the form

$$\alpha_7 - \alpha_1 > 0, \tag{24}$$

$$1 + \alpha_0 - \alpha_1\alpha_7 > 0, \tag{25}$$

$$\alpha_7 - \alpha_4\alpha_6 - \alpha_0\alpha_1 > 0, \tag{26}$$

$$\alpha_6 - \alpha_4\alpha_5 > 0, \tag{27}$$

$$\begin{aligned} &(\alpha_7 - \alpha_1)(1 + \alpha_0 - \alpha_1\alpha_7)(\alpha_7 - \alpha_4\alpha_6 - \alpha_0\alpha_1) \\ &\quad - (\alpha_7 - \alpha_4\alpha_6 - \alpha_0\alpha_1)^2 - (\alpha_7 - \alpha_1)^2(\alpha_6 - \alpha_4\alpha_5) > 0. \end{aligned} \tag{28}$$

Thus, at realization of the requirement (23) and not realization of at least one of inequalities (24)–(28) single equilibrium state of system (21) is unstable. In this case all trajectories of the system starting from a neighborhood of an origin of coordinate phase spaces, eventually abandon this neighborhood and due to dissipativity of the system, aspire to some limiting sets — attractors, which, as we shall see in the following, can be both regular and chaotic.

As the system of equations (21) is a non-linear system of the fourth order differential equations, all its further examinations will be done by means of numerical methods. The basic method of determination of solutions of the system (21) is the fourth or fifth order method of Runge–Kutta with the application of correcting procedure of Dormand–Prince [9], which ensures precision of the order $O(10^{-8})$ – $O(10^{-15})$. In the construction of phase portraits of the steady-state regimes the special attention was given to non-admission of their contortions by trajectories of transients process. For calculation of a spectrum of Lyapunov characteristic exponents (LCE) of attractors the algorithm of Benettin, etc. [4, 14, 21, 11] was applied. The influence of atypical trajectories on quantities of Lyapunov characteristic exponents was excluded. For construction of the Poincaré sections and mappings for attractors of the system the method of Hénon [10, 14] was applied, and for calculation of spectral densities the method of Filon was used [7].

Extensive numerical experiments were carried out with the purpose of finding the regions of exsistence of chaotic solutions. We assume that the generator works with the

following parameters:

$$\begin{gathered} E_g = 700V, \quad E_a = 2000V, \quad I_1 = 6.5 \times 10{-}5A/V, \quad I_3 = 5.184 \times X{\times}10{-}9A/V3, \\ D = 0.015, \quad R_a = 160\Omega, \quad R_c = 10\Omega, \quad L_c = 0.094H, \\ C_c = 1.0465\, mmF, \quad M_c = 0.275H, \quad M = 1H, \quad L = 100H. \end{gathered} \tag{29}$$

Here X is the dimensionless bifurcation parameter.

In this case the coefficients of system (21) are equal to

$$\begin{gathered} \alpha_0 = 0.995, \quad \alpha_1 = 0.0535, \quad \alpha_2 = 0.63 \times X, \quad \alpha_3 = 0.21 \times X, \\ \alpha_4 = -0.103, \quad \alpha_5 = -0.0604, \quad \alpha_6 = -0.12, \quad \alpha_7 = 0.01. \end{gathered} \tag{30}$$

We want to underline especially, that the values of parameters in formulas (29 - 30) correspond to real characteristics of LC-generators and piezoceramic transducers [2, 28]. For the chosen parameters of the system (21) it has a single zero equilibrium state which is unstable in the sense of Lyapunov.

Let's determine divergence ($\operatorname{div} F$) of the system (21). It is obvious, that it can be found using the formula

$$\operatorname{div} F = \alpha_1 + 2\alpha_2\zeta - 3\alpha_3\zeta^2 - \alpha_7. \tag{31}$$

As is seen from the formula (31) in a general case divergence will be a sign-alternating quantity. Taking into account parameters of system (30) it is possible to write the expression for divergence as

$$\operatorname{div} F = 0.63X\zeta(2 - \zeta) + 0.0435. \tag{32}$$

If the parameter X is positive then, up to 0.0435, divergence of system will be positive during those moments of time, when the phase variable ζ satisfies the inequality $2 > \zeta > 0$. Therefore, in cotrast to systems with a constant negative divergence, the question about local change in time of the phase volume of the system near a particular solution demands additional explanations. As is known [1], the given phase volume changes in time according to the expression

$$V(t) = V(t_0)e^{(\overline{\operatorname{div} F})t} = V(t_0)e^{(\lambda_1+\lambda_2+\lambda_3+\lambda_4)t}, \tag{33}$$

where $V(t)$ is the phase volume, λ_i is a Lyapunov characteristic exponent of an attractor, and in expression $\overline{\operatorname{div} F}$ the line denotes averaging in time. The carried out calculations have shown that the sum of Lyapunov characteristic exponents for all (examined further in the article) regular and chaotic attractors of system (21) will be negative. Therefore, negative will be averaged in time divergence of the system, though at some intervals of time it can be positive. It means, that all attractors of the systems (21) have zero limiting volumes.

Let's consider the bifurcations which are taking place in the system (21), when the parameter X is changing. We shall give special attention to the origin of chaotic attractors, their detailed exposition and scenarios of transitions from the regular regimes to the chaotic one. As is known, the basic practical criterion of existence of a chaotic attractor is the presence in a spectrum of LCE of at least one of the positive exponent [21, 14]. In Figure 3.1 a dependence of the maximal, distinct from zero, Lyapunov characteristic exponent on the parameter X is shown. Referring to Figure 3.1, there is a series

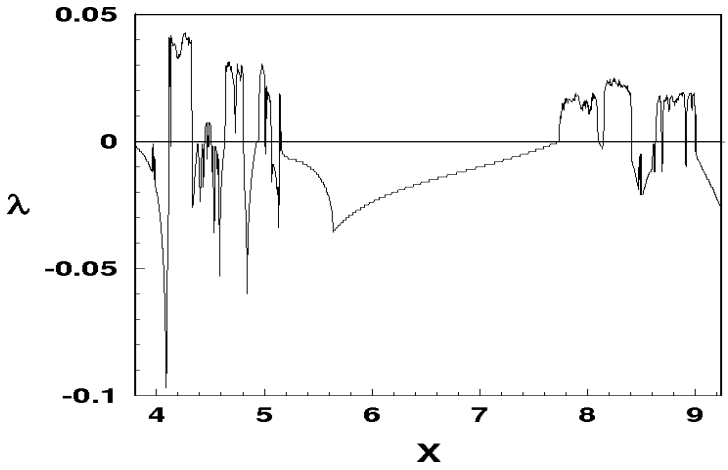

Figure 3.1: Dependence of the maximal Lyapunov characteristic exponent λ on X.

of X intervals in which the maximal Lyapunov exponent is positive. Hence, in these intervals there are chaotic attractors. Intersection points of this diagram with horizontal coordinate axis correspond to bifurcation values of parameter X.

In Figure 3.2 the phase-parametric characteristic of system (so-called bifurcation tree) is given. This characteristic is constructed as a function of coordinate ξ. Phase-parametric characteristics regarding other coordinates of the system are qualitatively similar to given in Figure 3.2. The light sites of this tree "crone" correspond to periodic regimes of the steady-state oscillations of the system (21), and densely blacked out - to chaotic. Points of a bifurcation, at which transition from regular periodic regime to the nonregular chaotic one occurs are precisely visible.

Let's now consider these changes of regimes in more details. At changing of the parameter X value in a segment $9.3 \geq X \geq 9.01$ in the system there is a stable limit cycle with the signature of a LCE spectrum which looks like ("0″, " −″, " −″, " −″). That is, the maximal Lyapunov exponent of the cycle is zero, and three others are negative. A three-dimensional projection of the phase portrait of this cycle, its Poincaré section by the plane $\beta = 0$ and the spectral density constructed in logarithmic scale, are given, accordingly, in Figure 3.3.a-b, Figure 3.4.a. The given figures are constructed at the value $X = 9.01$. Poincaré section and the spectral density have a structure typical for the regular regimes. A signal sent by the transducer to the medium in this case is periodic.

At $X = 9.005$ instead of a limit cycle as a result a saddle-knot or the tangential bifurcation a chaotic attractor arises in the system. In the signature of the LCE spectrum of the attractor the positive maximal exponent appears and it becomes: (" +″, "0″, " −″, " −″). In Figures 3.4.b, 3.5.a-b, 3.6.a the three-dimensional projection of the attractor phase portrait , its Poincaré section and mapping and the spectral density (Fourier spectrum) constructed at the value $X = 8.955$ are given, accordingly. Transition from the regular attractor to chaotic is carried out through an intermittency of the first type in the sense of Pomeau–Manneville [5]. When we move to a point of a bifurcation, the unstable cycle comes nearer to the limit cycle. In a point of bifurcations both cycles merge and disappear. Trajectories of system leave for remote fields of a

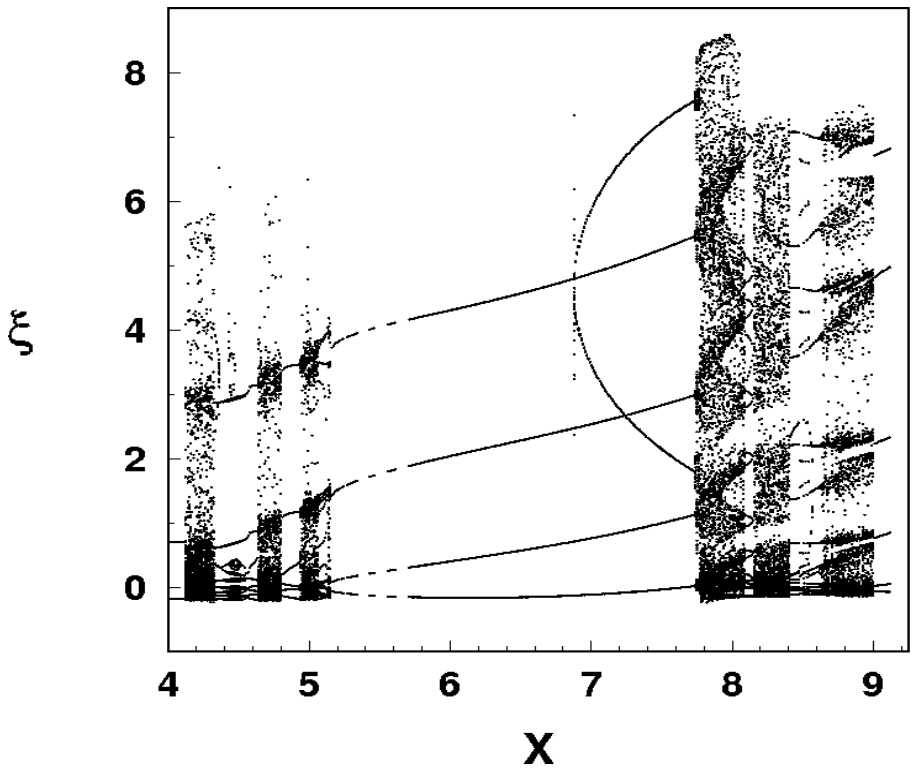

Figure 3.2: Phase-parametric characteristic of the system.

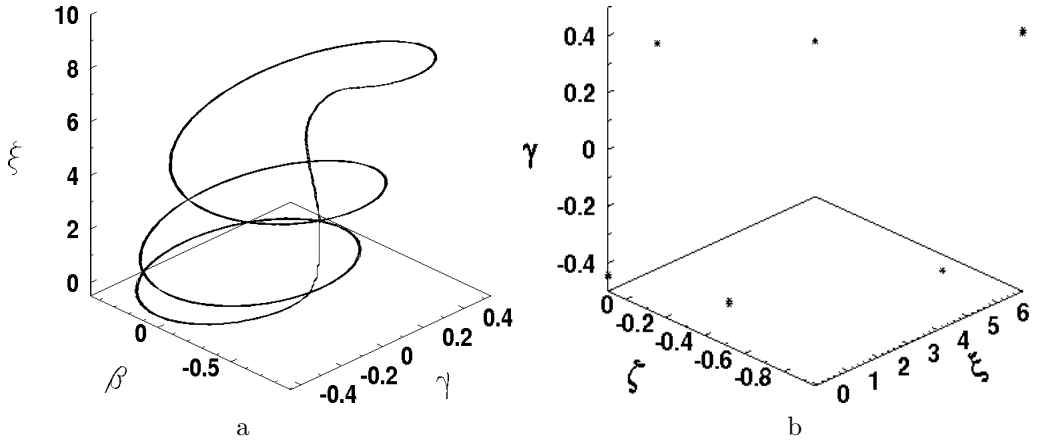

Figure 3.3: Projection of the phase portrait *(a)* and Poincaré section by the plane $\beta = 0$ *(b)* at $X = 9.01$.

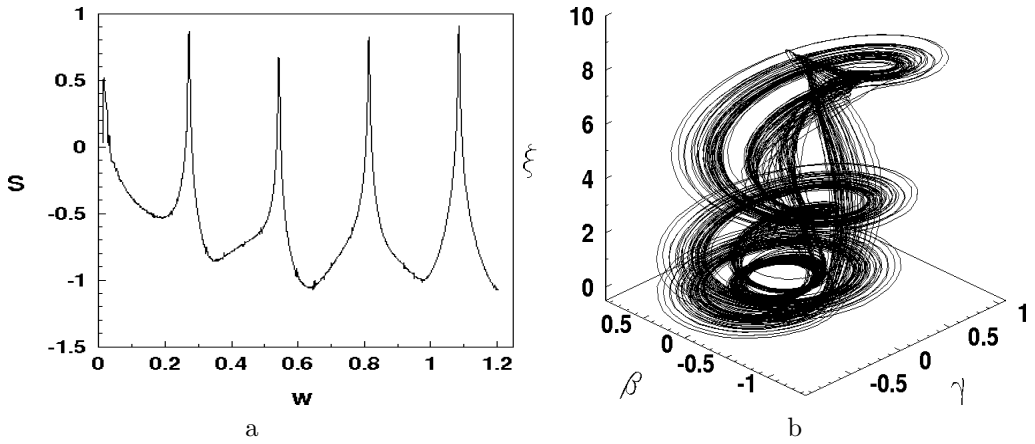

Figure 3.4: Spectral density at $X = 9.01$ *(a)* and the projection of the phase portrait at $X = 8.955$ *(b)*.

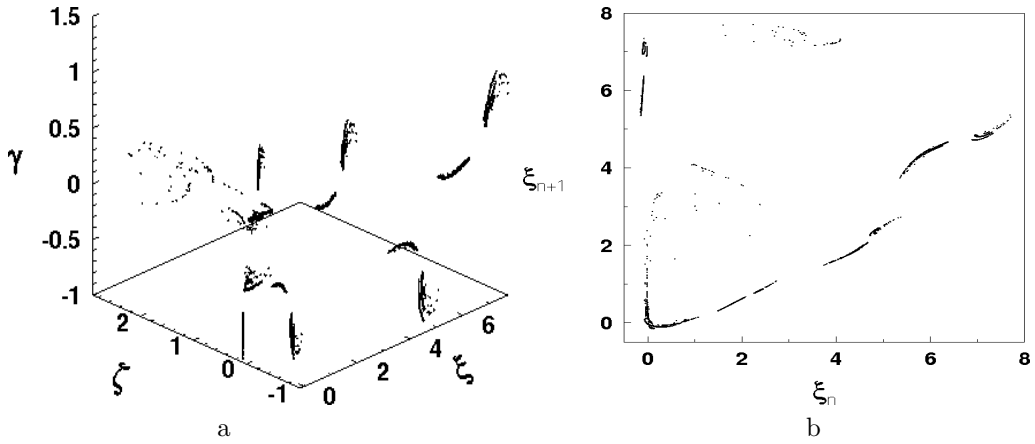

Figure 3.5: Poincaré section by the plane $\beta = 0$ *(a)* and mapping *(b)* at $X = 8.955$.

phase space. Then, because the system (21) is stable in the sense of Lagrange (by its dissipativity) and in the sense of Poisson (as a regime is steady-state) and is unstable in the sense of Lyapunov (a positive Lyapunov exponent exists), a process of reinjections happens, when returnings of trajectories to neighborhood of the vanished limit cycle happen, then again they leave and return end so on. Laminar phase of this intermittency is the motion in enough small neighborhood of the vanished limit cycle, and turbulent phase is unpredictable roamings around the coils of a spiral chaotic attractor (see Figure 3.4.b). Transition to chaos through an intermittency is also testified by the structure of a bifurcation tree in a neighbourhood of the point $X = 9.01$.

Poincaré section and mapping represent some chaotic point sets, which are grouped inside of several domains having quasiribbon structure. The view of Poincaré mapping shows, that the system (21) can be roughly enough approximated by means of the one-dimensional mapping that will essentially simplify its investigation. The view of this mapping (which can be substituted by a set of one-dimensional parabolic and horseshoe-

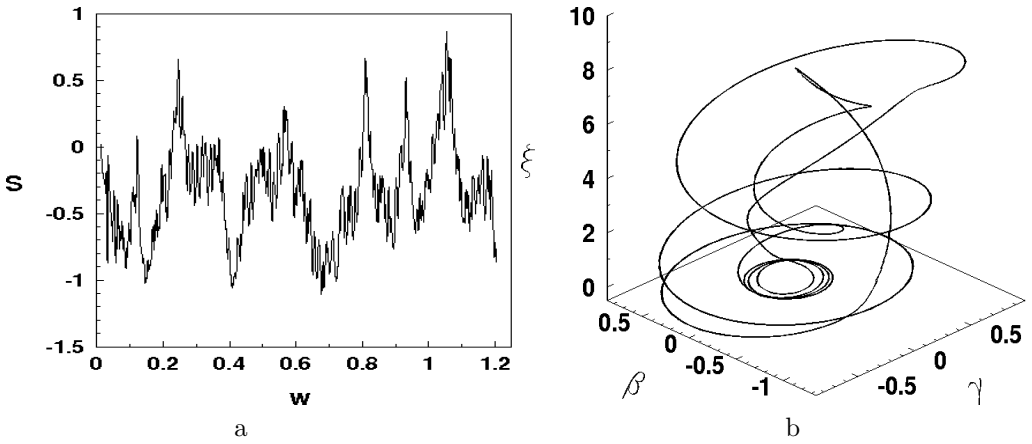

a b

Figure 3.6: Spectral density at $X = 8.955$ *(a)* and a projection of a phase portrait at $X = 8.41$ *(b)*.

shaped lines) is one more proof that the system has a chaotic regime [14]. A spectrum of an attractor is continuous, but with apparent enough peaks. A continuity of Fourier spectrum also testifies a chaotic character of the given attractor. Chaotic attractors of such type exist in the system (21) at $9.005 \geq X \geq 8.645$. A signal generated by the transducer to the medium at such X will be chaotic.

Now consider several types of the attractors existing in the system (21). At $8.645 > X \geq 8.41$ a stable limit cycle exists in the system. A projection of a phase portrait of such cycle is given in Figure 3.6.b. This cycle has more complex structure, than the cycle given in Figure 3.3.a. Besides it has approximately six times larger period, than a cycle given in Figure 3.3.a. At the value $X \simeq 8.405$ this cycle disappears, due to a tangent bifurcation, and the chaotic attractor of new type is born (whose projection of the phase portrait is constructed at value $X = 8.25$ and is given in Figure 3.7.a). Transition from the regular attractor to the chaotic one, as before, is carried out through the first type intermittency in the sense of Pomeau–Manneville according to the described above scenario. However, unlike the previous described chaotic attractor (Figure 3.4.b), here we have a more continuous covering by turbulent splashes of an attractor trajectories of its phase volume. The signature of the LCE spectrum of this chaotic attractor looks like: ("+", "0", "−", "−").

In Figure 3.7.b Poincaré section of this attractor is shown. It represents a chaotic point set the number of which constantly increases with the time of numerical integration time of the system. However for this type of chaotic attractors its Poincaré section loses quasiribbon structure.

In Figure 3.8.a one more important characteristic of chaotic attractors is shown, namely a distribution of an invariant measure of Krylov–Bogolyubov on the attractor phase portrait. The given figure is constructed by so-called technique of coding by grey color tones as stated in [14]. The invariant measure is a quantitative characteristic of the residence time of a representation point of attractor trajectories in the given region of the phase volume. More dark parts in the figure correspond to regions in which representation point of trajectories spends a majority of time. As is apparentl from Figure 3.8.a, the trajectories spend the largest part of time in the neighborhoods of

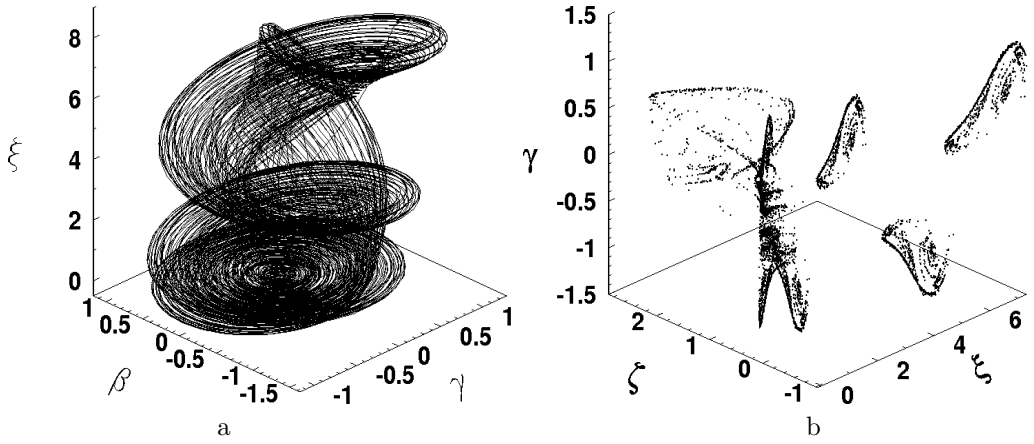

Figure 3.7: Projection of the phase portrait *(a)* and Poincaré section by the plane $\beta = 0$ *(b)* at $X = 8.25$.

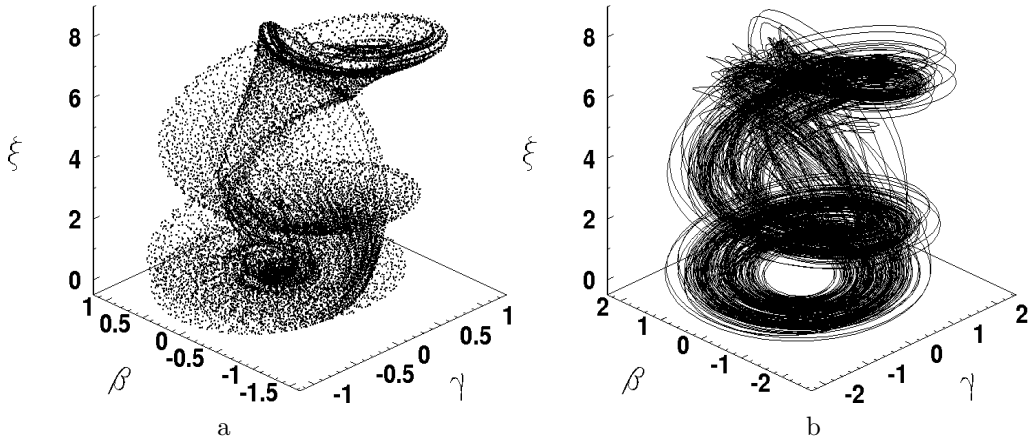

Figure 3.8: Distribution of an invariant measure at $X = 8.25$ *(a)* and projection of the phase portrait at $X = 7.85$ *(b)*.

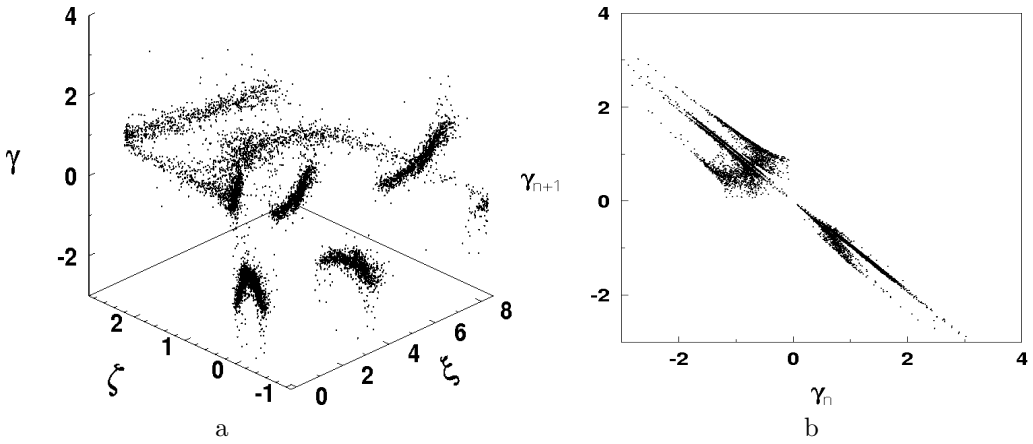

Figure 3.9: Poincaré section by the plane $\beta = 0$ *(a)* and mapping *(b)* at $X = 7.85$.

the vanished limit cycle that is the testimony of larger duration of laminar phases in comparison with the turbulent ones. Moreover, this figure is one more verification of realization of the intermittency scenario at transition from the regular regime to chaotic.

At the value $X = 7.86$ an extremely interesting bifurcation of a type "chaos–chaos" happens, when as a result of the complex mechanisms of interactions of a chaotic attractor with the saddle limiting cycles existing in pool of its attraction, in the system (21) an attractor arises whose signature of LCE spectrum looks like ("+", "+", "0", "−"). This attractor has two positive Lyapunov exponents. Such attractor is called hyper-chaotic [14]. Such type attractors exist only in dynamic systems, dimensionality of which in phase space is more or equal to four, and are characterized by the presence in LCE spectrum of not less than two positive Lyapunov exponents. Presence of two positive exponents indicates the existence in a phase space of two directions in which the close phase trajectories of an attractor diverge. All above-considered chaotic attractors have only one direction of divergence of the close phase trajectories. In Figure 3.8.b the projection of a phase portrait of a hyper-chaotic attractor is shown for $X = 7.85$. A phase portrait of such attractor has a "hole" in its lower ring spirals.

In Figures 3.9.a-b the Poincaré section and mapping of a hyper-chaotic attractor are shown. As can be seen the observed structures have more complicated chaotic point sets than those in (Figures 3.5.a-b and Figure 3.7.b). The one-dimensional approximation of mapping of Poincaré ia out of the question. Further in Figures 3.10.a-b the distribution of invariant Krylov-Bogolyubov's measure and the spectral density of the hyper-chaotic attractor are given, accordingly. As is apparent from Figure 3.10.a, now the hyper-chaotic attractor possesses more uniform distribution of invariant measure than the attractor existing at $X = 8.25$. Distribution of the spectral density of the hyper-chaotic attractor is , as before, continuous, however in it separate peaks practically disappear. Hyper-chaotic attractors exist in rather small interval of changing of the parameter X, namely, $7.86 \geq X \geq 7.745$. At the further decreasing of X they disappear and in the system a stable limit cycle arises again.

As can be seen in Figure 3.1, there are some more intervals of the parameter X changing in which chaotic attractors exist. The further examinations made possible to find out still some more transitions from the regular motions to chaotic through

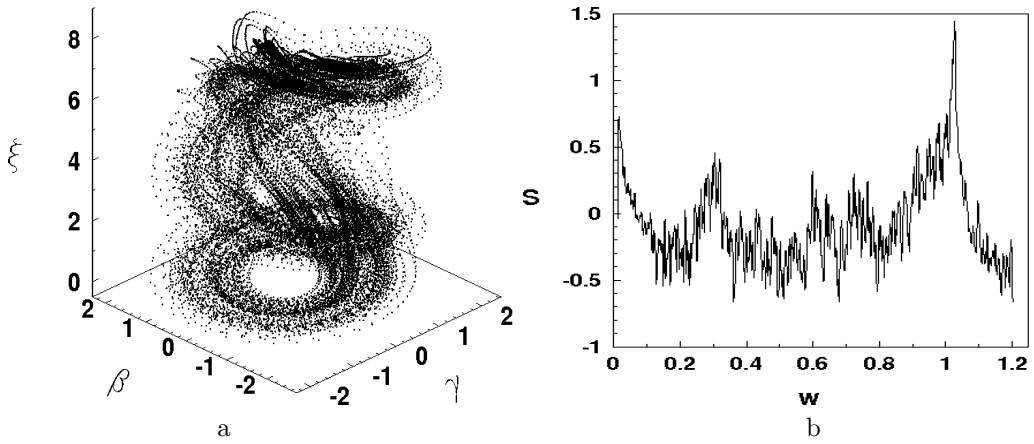

Figure 3.10: Distribution of an invariant measure *(a)* and a spectral density *(b)* at $X = 7.85$.

intermittency. Besides, transitions to chaos have been discovered through cascade of bifurcations of doubling of a period [6].

Let's consider one more type of the chaotic attractor discovered in system (21). Attractors of such type exist in system at $4.325 \geq X \geq 4.115$. Transition from the regular condition to chaotic here, as well as in several previous cases, is carried out under the scenario of an intermittency of the first type. The signature of LCE spectrum of such attractor looks like: (" $+''$, "$0''$, " $-''$, " $-''$). In Figures 3.11.a-b, 3.12.a-b the three-dimensional projection of the attractor phase portrait, its Poincaré section by the plane $\beta = 0$, Poincaré mapping and a spectral density constructed at the value $X = 4.255$are shown respectively . As can be seen from these figures, the phase portrait of a chaotic attractor has varied noticeably, on which merging of rings of its spirals has happened. Amplitudes of oscillations of phase variables have decreased. But, at the same time, as is apparent from Figure 3.1, the maximal Lyapunov characteristic exponent for this attractor is approximately twice as large as corresponding exponents for the above chaotic attractors. It testifies to much greater velocity of divergence of the close phase trajectories. Disposition of points in Poincaré cross-section has considerably varied, however, it is still some chaotic point set. Mapping of coordinate ξ vaguely resemble corresponding mapping, given in Figure 3.5.b, however, a disposition of points on mapping, given in Figure 3.12.a, testifies about impossibility of any one-dimensional approximation in this case. Fourier spectrum of an attractor (Figure 3.12.b) has continuous structure and is characterised by the absence of peaks.

The comparative analysis of behaviour of the system "generator – transducer" in the case of an ideal excitation, when we neglect influence of a transducer on functioning of the generator, attracts a significant interest. This is the case of zero coefficient α_4 in the system of equations (21). In Figure 3.13.a-b phase portraits are given for attractors of the systems (21) constructed at $\alpha_4 = 0$, $X = 8.25$ (Figure 3.13.a) and $\alpha_4 = 0$, $X = 7.85$ (Figure 3.13.b). In both cases attractors of system are limit cycles. Meanwhile under the nonideal excitation, which always takes place by virtue of the law of conservation of energy, the system will be in chaotic (at $X = 8.25$) or in hyper-chaotic (at $X = 7.85$) regimes. Moreover, the case of an ideal excitation is characterised by appreciable diminution of vibration amplitudes of phase variables, especially of the variables

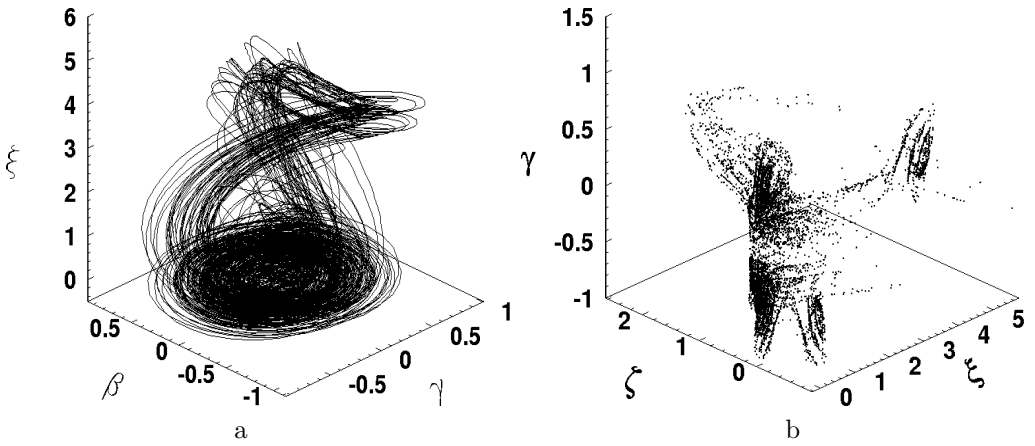

Figure 3.11: Projection of a phase portrait *(a)* and Poincaré section by the plane $\beta = 0$ *(b)* at $X = 4.255$.

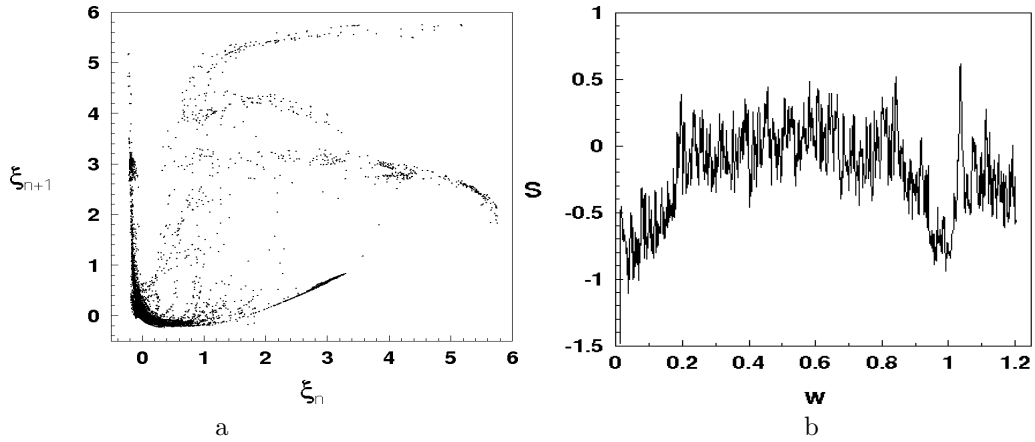

Figure 3.12: Poincaré mapping *(a)* and spectral density *(b)* at $X = 4.255$.

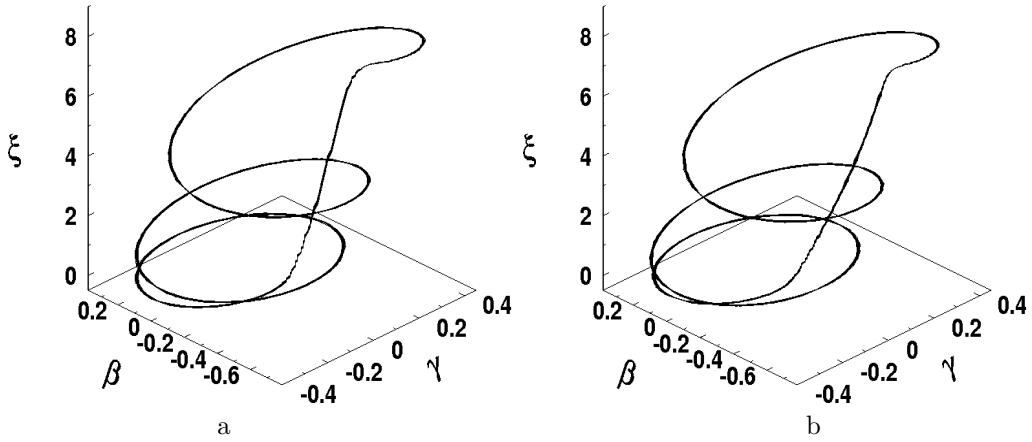

Figure 3.13: Projection of a phase portrait at $X = 8.25$, $\alpha_4 = 0$ *(a)* and projection of a phase portrait at $X = 7.85$, $\alpha_4 = 0$ *(b)*.

β, γ which describe oscillations of the transducer. Thus, the neglection of nonidealness of excitation leads to the significant errors in exposition of process of interaction of transducer and generator both quantitative, and, what is more essential, qualitative. For example, instead of expected periodic regimes of interaction the system actually will be in a hyper-chaotic regime.

Further an examination of the bifurcations which are taking place at a changing of parameter α_4 (which, as it has just been noted, characterizes interaction between transducer and generator) has been carried out. In the computer experiments values of parameters of system were defined by formulas (30) except for the parameter α_4 which was taken as bifurcation one and was variable. For parameter X it was supposed, that $X = 7.82$. Such value of parameter X previously corresponded to the case of hyper-chaos in the system.

In Figure 3.14 dependence of the maximal, distinct from zero, Lyapunov characteristic exponent of the system λ on the values α_4 is given. As is apparent from the figure, there are intervals of α_4 in which values of λ will be positive. In these intervals the system has chaotic attractors. At $\alpha_4 = 0$ the system (21) has stable limited cycle, whose phase portrait practically coincides with phase portrait of a cycle given in Figure 3.13.b. However, already at very small changing of α_4 value, namely at $\alpha_4 = -0.004$, the maximal Lyapunov characteristic exponent becomes positive, that testifies about origin of the chaotic attractor. As we see, even very small interaction between subsystems, the generator and the transducer, leads to occurrence of chaos.

Let's consider the bifurcations happening in the system (21) at increasing of α_4. At $\alpha_4 = -0.138$ in system a stable limit cycle exists. Further, at increase of value α_4, on very small interval $(-0.138, -0.13515)$ in the system there is a cascade of bifurcations of period doubling, which comes to an end with origin of a chaotic attractor at $\alpha_4 = -0.1351$. A projection of a phase portrait of this attractor, its Poincaré section and mapping, and also distribution of the spectral density, constructed at $\alpha_4 = -0.135$, are given respectively in Figures 3.15.a–b, 3.16a–b.

Here the transition from the regular regime to chaotic here is carried out in correspondence with Feigenbaum's scenario [6]. We would like to emphasize, that this attractor is

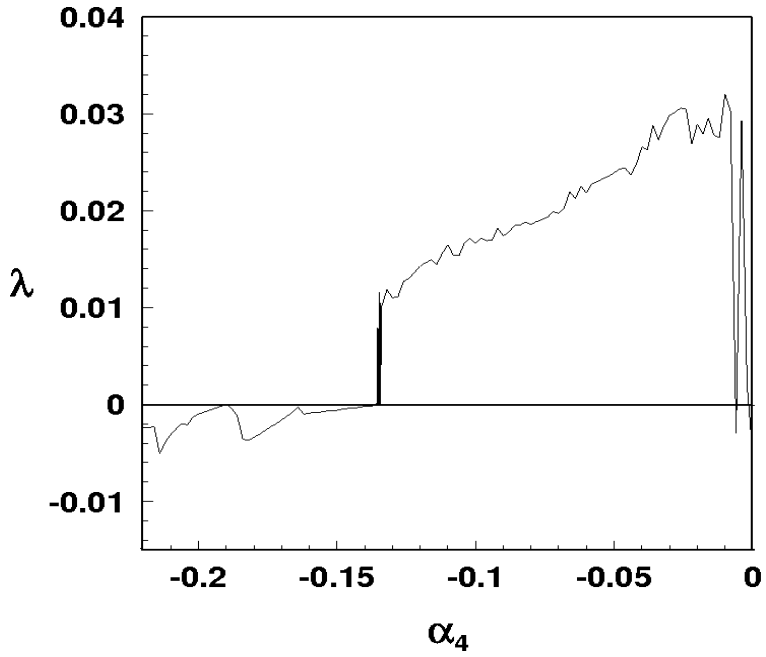

Figure 3.14: Dependence of the maximal Lyapunov characteristic exponent λ on the parameter α_4.

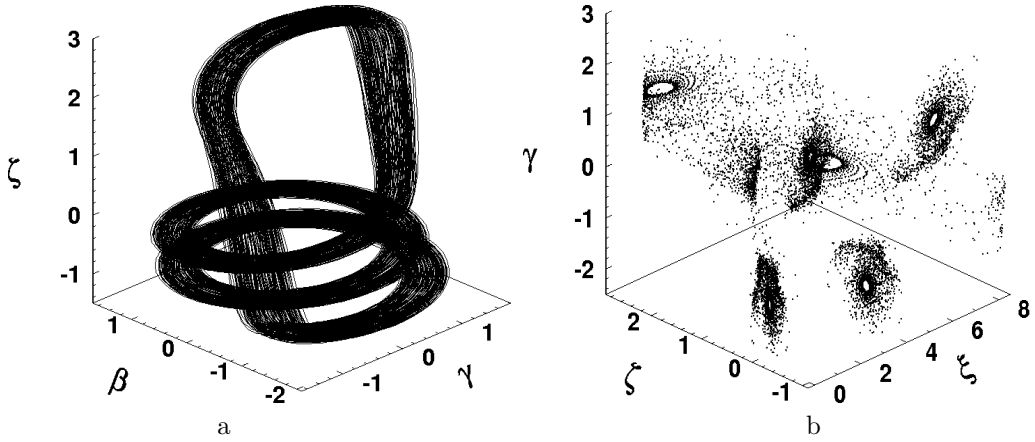

Figure 3.15: Projection of a phase portrait *(a)* and Poincaré section by the plane $\beta = 0$ *(b)* at $\alpha_4 = -0.135$.

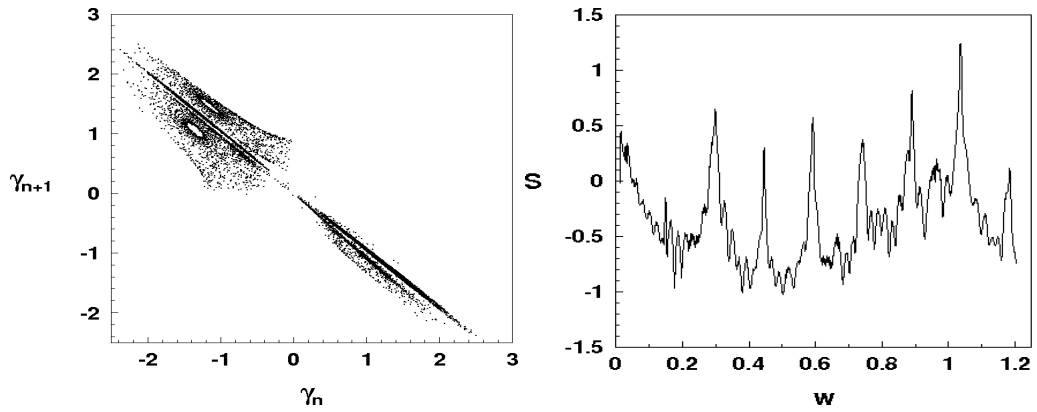

Figure 3.16: Mapping *(a)* and spectral density *(b)* at $\alpha_4 = -0.135$.

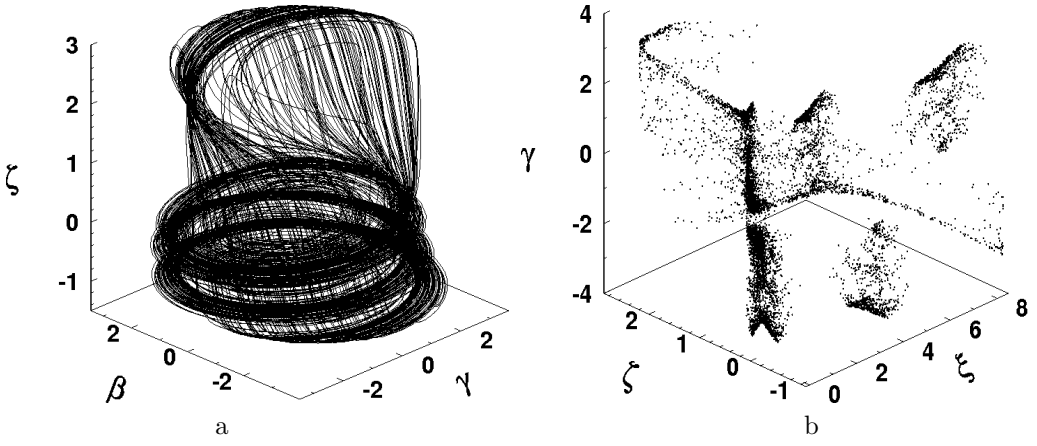

Figure 3.17: Projection of a phase portrait *(a)* and Poincaré section by the plane $\beta = 0$ *(b)* at $\alpha_4 = -0.025$.

hyper-chaotic as it has two positive Lyapunov characteristic exponents. Phase portrait of this attractor noticeably differs from the hyper-chaotic attractor considered above. At the same time Poincaré section and mapping possess some qualitative simularity with the cases of hyper-chaos shown in Figure 3.9 a–b. Essential differences are found in Fourier spectrum of the given attractor. It is continuous, but, at the same time, the spectrum peaks are precisely pronounced. They are "the memories" about harmonics of vanished limit cycles. This the hyper-chaotic attractor exists in system in the very small interval $(-0.1351, -0.1348)$ of α_4. Then in the system there is "a window of periodicity" which again is replaced by hyper-chaotic attractor at $\alpha_4 = -0.1344$. Arising attractor is qualitatively similar to a hyper-chaotic attractor, given in Figure 3.8.b. Further increase of α_4 leads to the bifurcation "hyper-chaos — chaos", as a result of which, at $\alpha_4 = -0.058$, a chaotic attractor arises. The signature of LCE spectrum of given attractor looks like: ("+", "0", "−", "−"). In Figure 3.17.a a projection of a phase portrait and Poincaré section of attractors of this type constructed at value $\alpha_4 = -0.025$ are given, accordingly. Chaotic attractors similar to that given in Figure 3.17 exist in the system (21) at $-0.058 \leq \alpha_4 \leq -0.004$. Then, at $\alpha_4 > -0.004$, the regular attractor — a limit cycle arises again in the system.

4 Conclusion

Thus, in the present work a series of new effects has been discovered, caused by process of interaction of oscillation regimes in piezoceramic transducer and setting electric generator, and obtained on the basis of the constructed new mathematical model.

In the given deterministic system some types of chaotic attractors were revealed, including the hyper-chaotic one. It is shown, that the system possesses a significant variety of existing in it steady-state regimes of interaction, their properties, and also scenarious of transition from the regular conditions to chaotic. It was established that existence of the deterministic chaos in the system is caused only by interaction between subsystems (generator and transducer), instead of their independent properties.

These effects are applicable at the analysis of the regular and chaotic regimes of functioning of electrodynamic, electromagnetic and piezoceramic vibrators with the limited excitation.

Acknowledgments

The authors are very grateful to Prof. A.M. Samoilenko for extensive discussions and illuminative conversations.

References

[1] Anishchenko, V.S., Astakhov, V.V, Nieman, A.B, Vadivasova, T.E. and Schimansky–Geier, L. *Nonlinear Dynamics of Chaotic and Stochastic Systems*. Springer, Berlin, 2003.

[2] Auld, B.A. *Acoustic Fields and Waves in Solids*. John Wiley & Sons, New York, 1973.

[3] Bazenov, V.M. and Ulitko, A.F. Examination dynamic behaviour of a piezoceramic stratum at instantaneous electrical loading. *Appl. Mech.* **11**(1) (1975) 22–27. [Russian]

[4] Benettin, G., Galgani, L., Strelcyn, J.M. Kolmogorov entropy and numerical experiments. *Phys. Rev. A*. **14** (1976) 2338–2342.

[5] Berge, P., Pomeau, Y. and Vidal, C.H. *Order within chaos.* John Wiley & Sons, New York, 1984.

[6] Feigenbaum, M.J. Quantative universality for a class of nonlinear transformations. *J. Stat. Phys.* **19**(1) (1978) 25–52.

[7] Filon, L.N.G. On a quadrature formula for trigonometric integrals. *Proc. R. Soc. Edinburgh* **49** (1929) 38–47.

[8] Grinchenko, V.T., Ulitko, A.F. and Shulga N.A. *Electroelasticity.* Naukova Dumka, Kiev, 1989. [Russian]

[9] Hairer, E., Norsett, S.P. and Wanner, G. *Solving ordinary differential equations. Nonstiff problems.* Springer–Verlag, Berlin, 1987.

[10] Hénon, M. On the numerical computation of Poincaré maps. *Physica. D.* **5** (1982) 412–415.

[11] Khaki–Sedigh, A., Ataei, M., Lohmann, B. and Lucas, C. Adaptive Calculation of Lyapunov Exponents from Time Series Observations of Chaotic Time Varying Dynamical Systems. *Nonlinear Dynamics and Systems Theory* **4** (2004) 145–159.

[12] Kononenko, V.O. *Vibrating systems with a limited power supply.* Iliffe Books, London, 1969.

[13] Kononenko, V.O. and Krasnopolskaya, T.S. The vacuum tube generator in to system of excitation of mechanical oscillations. *Vibrotechnics* **28** (4) (1977) 105–120. [Russian]

[14] Kouznetsov, S.P. *Dynamic chaos.* Physmatlit, Moscow, 2001. [Russian]

[15] Krasnopolskaya, T.S. Independent excitation mechanical oscillations by the electrodynamic vibrator. *Sov. Appl. Mech.* **13**(2) (1977) 108–113.

[16] Krasnopolskaya, T.S. and Shvets, A.Yu. Chaos in dynamics of machines with a limited power-supply. In: *8-th World Congr. on the theory of machines and mechanisms.* Prague: Czechoslovak Acad. Sci., Vol. 1, 1991, 181–184.

[17] Krasnopolskaya, T.S. and Shvets, A.Yu. Chaos in vibrating systems with limited power-supply. *Chaos* **3** (1993) 387–395.

[18] Krasnopolskaya, T.S. and Shvets, A.Yu. Chaotic surface waves in limited power-supply cylindrical tank vibrations. *J. Fluids and Structures* **8** (1994) 1–18.

[19] Krasnopolskaya, T.S. Acoustic chaos caused by Sommerfeld effect. J. Fluids and Structures **8** (1994) 803–815.

[20] Martynyuk, A.A. Stability of Dynamical Systems in Metric Space. *Nonlinear Dynamics and Systems Theory* **5** (2005) 157–168.

[21] Neimark, J.I. and Landa, P.S. *Stochastic and chaotic oscillations.* Nauka, Moscow, 1987. [Russian]

[22] Rayleigh, W. *Theory of Sound.* Macmillan, London, 1877.

[23] Perel, V.Y. and Palazotto, A.N. A Nonlinear Model of Composite Delaminated Beam with Piezoelecric Actuator, with Account of Nonpenetration Constraint for the Delamination Crack Faces. *Nonlinear Dynamics and Systems Theory* **4** (2004) 161–194.

[24] Sommerfeld, A. Beitrage zum dynamischen ausbau der festigkeislehre. *Zeitschrift des Vereins Deutscher Ingenieure* **46** (1902) 391–394.

[25] Timoshenko, S. *Vibration Problems in Engineering.* Van Nostrand Co., New York, 1928.

[26] Ulitko, A.F. The Conjugate undular processes in piezoceramic skew fields at the electrical discharge. *Acoustical Bull.* **2**(1) (1999) 60–73. [Russian]

[27] Ulitko, A.F. *Vector Decomposition in the Space Theory Elasticities.* Akademperiodica, Kiev, 2002. [Russian]

[28] Zharii, O.Yu. Normal mode expansions in dynamic electroelasticity and their application to electromechanical energy conversion. *J. Acoust. Soc. Am.* **91**(1) (1992) 57–68.